CHAPTER II

THEORY AND LITERATURE

Perovskite Structure

Since the ferroelectric properties of barium titanate were reported by Von Hippel in 1945, ABO_3 compound with the perovskite structure have been studied extensively [27, 28]. These studies have resulted in the discovery of many new ferroelectric and piezoelectric materials. Most of the literatures on perovskite-type compounds have concentrated on these properties.

Perovskite is the name of the mineral calcium titanate ($CaTiO_3$). Most of the useful piezoelectric (ferroelectric) ceramics, such as bismuth sodium titanate ($Bi_xNa_{1-x}TiO_3$), barium titanate ($BaTiO_3$), lead titanate ($PbTiO_3$), lead zirconate titanate ($PbZr_{1-x}Ti_xO_3$), lead lanthanum zirconate titanate (PLZT), potassium niobate ($KNbO_3$), potassium sodium niobate ($KNa_xNb_{1-x}O_3$), have a perovskite structure. These oxide ceramics have the general chemical formula ABO_3, where O is oxygen in the centers of the faces. Arepresents a cation with a larger ionic radius on the corners, and Brepresents a cation with smaller ionic radios in the center of the body [29, 30, 31]. Figure 1 shows a cubic ABO_3perovskite-type unit cell and three–dimensional network of BO_6- octrahedral. A sites are occupied by Bi^{2+}, Ba^{2+},Pb^{2+}, K^+or Na^+ions, and B sites by Ti^{4+}, Zr^{4+}, Nb^{5+}or Ta^{5+}ions.

Binary or ternary solid solutions of more than one of these simple perovskites allows for the creation of more complex perovskites. Essentially, multiple elements split the occupancy of the A or B site and must average out to the appropriate charge for that site according to the same principles used in the case of the three simple perovskite types listed above. The high stability of the perovskite structure allows for highly complex charged compensated compositions to form. The general formula for complex perovskites can be written as $(A'A'')^{XII}(B'B'')^{VI}X_3$. While many of the complex perovskite families are known to be relax or ferroelectric, there has been significant success in modifying ferroelectric compositions such as $(Bi_{0.5}{}^{3+}K_{0.5}{}^{1+})Ti0_3$, $(Bi_{0.5}{}^{3+}Na_{0.5}{}^{1+})Ti0_3$, and many combinations of these two. Another highly investigated

system to be covered is $(K_{0.5}^{1+}Na^{1+})(Nb_x^{5+}Ta_{1-x}^{5+})O_3$, with even further elements being introduced to enhance the piezoelectric properties.

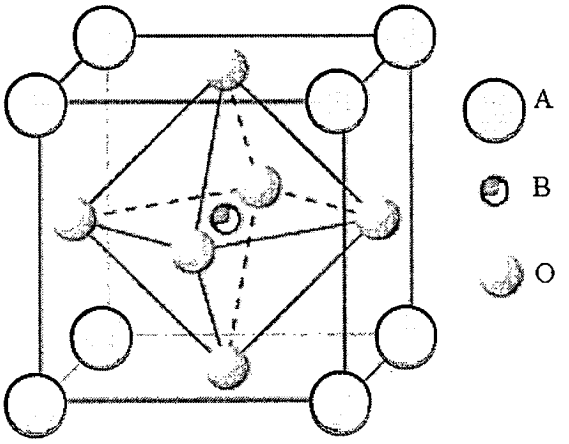

Figure 1 The perovskite structure as an ABO_3perovskite-type unit cell [27]

Piezoelectricity

Piezoelectricity was discovered in 1880 by Jacques and Pierre Curie during their systematic study of the effect of pressure on the generation of aelectrical charge by crystals such as quartz, zincblend, and tourmaline [29, 30, 32]. The name "piezo" is derived from the Greek, meaning "to press", hence piezoelectricity is the generation of electricity as a result of mechanical pressure. Many piezoelectric materials are not ferroelectric but all ferroelectrics are piezoelectric. Two effects are operative in piezoelectricity. The direct effect is identified with the phenomenon whereby an electrical charge (polarization) is generated from mechanical stress, whereas the converse effect is associated with the mechanical movement generated by the application of an electrical field. Both of these effects are illustrated in Figure 2

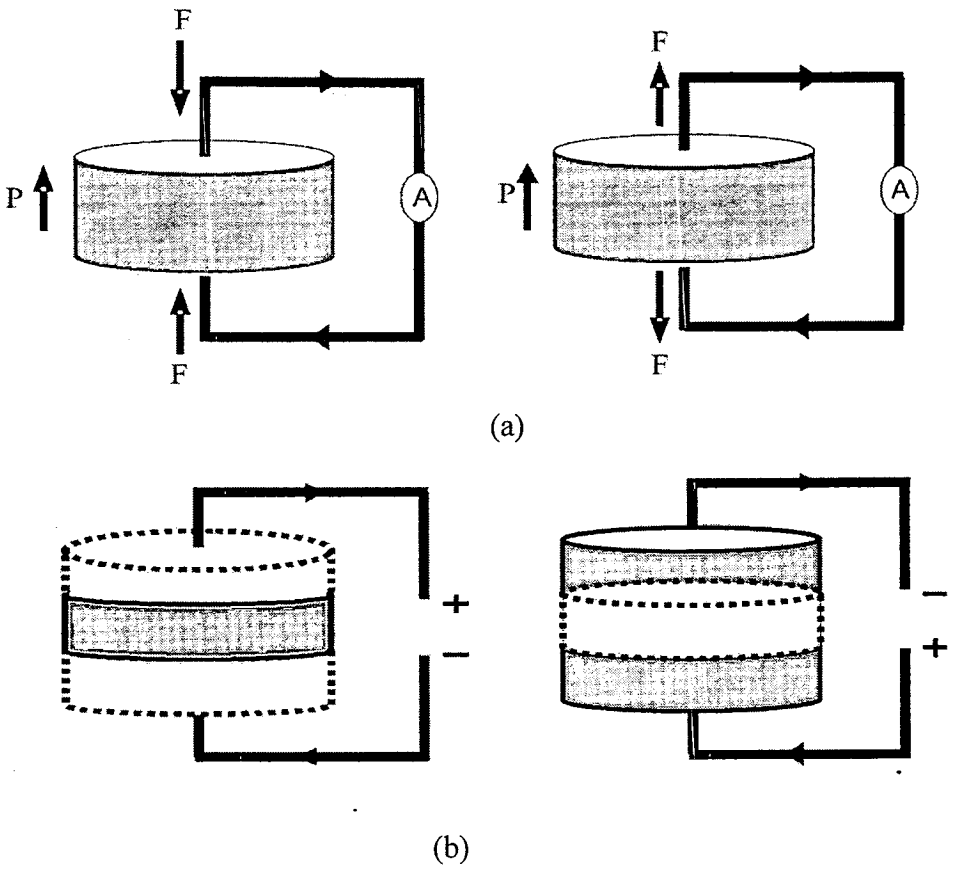

Figure 2 Piezoelectric effects in ferroelectric ceramics
(a) direct effect (b) converse effect [29]

The basic equations that describe these two effects in regard to electric and elastic properties are

$$D = dT + \varepsilon^T E \tag{1}$$

$$S = s^E T + dE \tag{2}$$

Where D is the dielectric displacement (consider it equal to polarization), T the stress, E the electric field, S the strain, d a piezoelectric coefficient, s the material compliance (inverse of modulus of elasticity), and ε the dielectric constant(permittivity). The subscripts indicate a quantity held constant: in the case of ε^T, the stress is held constant, which means that the piezoelectric element is

mechanically unconstrained, and, in the case of s^E, the electric field is held constant, which means the electrodes on the element are shorted together.

Ferroelectrics

Ferroelectricity is a phenomenon which was discovered by Valasek in 1921 [33]. It has become customary to call ferroelectricity the phenomenon exhibited by these crystals and ferroelectric the crystal themselves. This is due to a formal similarity of the ferroelectric phenomenon with that of ferromagnetism. The similarity is mainly phenomenological. As ferromagnetic materials exhibit a spontaneous magnetization and hysteresis effects in the relationship between magnetization and magnetic field, ferroelectric crystals show a spontaneous electric polarization and hysteresis effects in the relation between the dielectric displacement and the electric field. This behavior is mostly observed in certain temperature regions below by transition temperature (Curie temperature) where those crystals above are this transition temperature are no longer ferroelectric.

The crystal symmetries of the paraelectric and ferroelectric phase are an important factor in displaying the ferroelectric behavior of the materials. The lattice structure described by the Bravais unit cell of the crystal governs the crystal symmetry. Though there are thousands of crystals in nature, they all can be grouped together into 230 microscopic symmetry types or space groups based on symmetry elements. It can be shown by the inspection of the 230 space groups that there are just 32 point groups. As shown in Figure 3, the 32 point groups can be further classified into (a) crystal having a center of symmetry and (b) crystals which do not possess a center of symmetry (noncentrosymmetric). There are 21 classes of noncentrosymmetric, a necessary condition for piezoelectricity to exist, and only 20 are piezoelectric. Among these 20 point groups, only 10 can display a spontaneous polarization, which is designated as pyroelectric. A subgroup of the spontaneous polarized pyroelectric is a category of materials known as ferroelectrics. Ferroelectrics are a special class of materials in which a permanent electric dipole can be reoriented between equilibrium states by the external electric field. Continuing Valasek's analogy between ferroelectric and ferromagnetic, the dependence of the polarization on an applied electric field can be seen by polarization versus electric field i.e. (P-E)

hysteresis loop as shown in Figure 4. The hysteresis loop is typically observed using the simple circuit described by Sawyer-Tower [35]. One parameters obtained from the hysteresis loop measurement, the remnant polarization (P_r) is the crystal spontaneous polarizes along one of the allowed direction without applied electric field. The field required to reverse the polarization is known as the coercive field (E_c). Ferroelectric materials are divided into two main categories as normal and relaxor ferroelectrics.

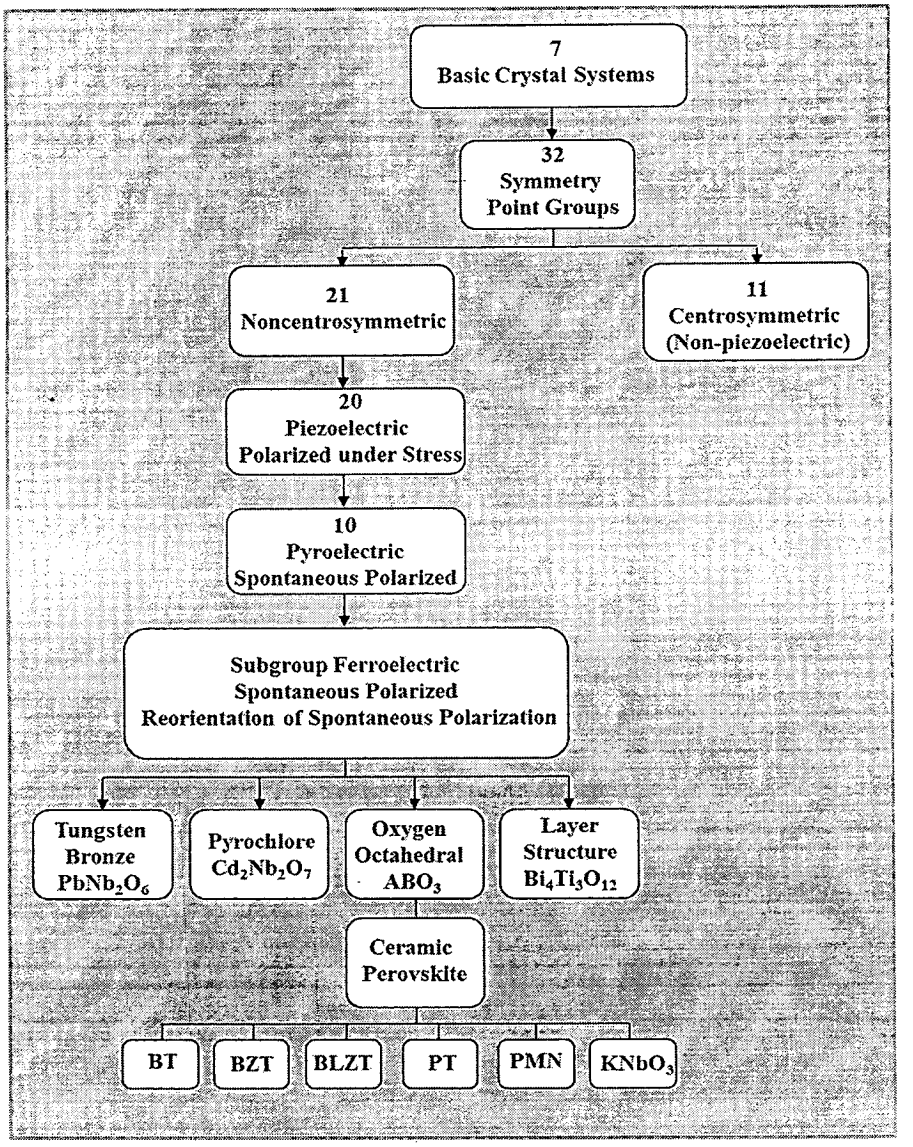

Figure 3 Interrelationship of piezoelectric and subgroups on the basis of symmetry [33]

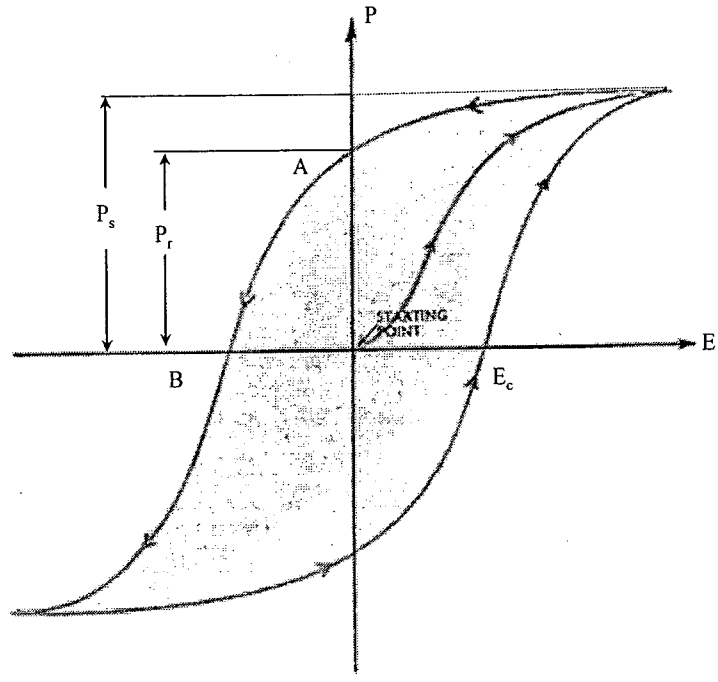

Figure4 A ferroelectric hysteresis loop [33]

Normal ferroelectric

Normal ferroelectric materials have a sharp phase transition which occurs at a specific temperature called the Curie temperature, T_c. The T_c is the temperature which the crystal structure transforms from the paraelectric state into the ferroelectric state and vice versa [36, 37, 38, 39]. In the paraelectric state, the dielectric permittivity obeys the Curie-Weiss law:

$$\varepsilon_r = \frac{C}{T - T_0} \tag{3}$$

Where C is the Curie-Weiss constant, T is the temperature and, T_0 is the Curie-Weiss temperature. The Curie temperature (T_c) and the Curie-Weiss temperature (T_0) should not be confused. The Curie temperature is the actual transformation temperature, but the Curie-Weiss temperature is found by extrapolating the plot of the Curie-Weiss law, as shown in Figure 5. The Curie temperature and Curie-Weiss temperature typically differ by only a small amount that depends on the type of phase formation the material undergoes. The Curie-Weiss temperature

can be as much as ten degrees lower than the Curie temperature for first-order phase transformations and the two can be nearly equal for second-order phase transformations (first order phase transformations are those in which the first derivative of the free energy, with respect to temperature, is discontinuous; second order phase transitions are those in which the second derivative is discontinuous)

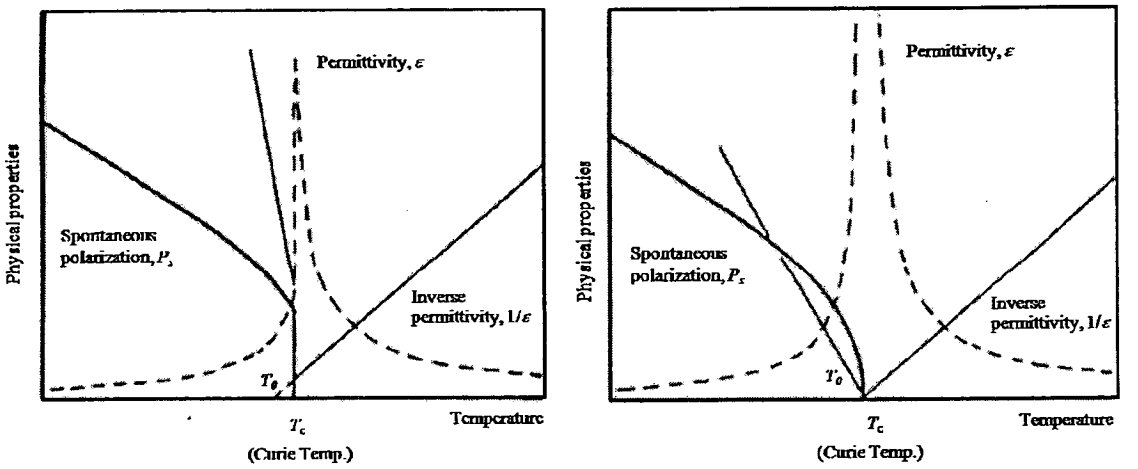

Figure 5 Phase transition in a ferroelectric (a) first order and (b) second order [36]

Relaxor ferroelectric

The relaxor behaviorswere recognized by Cross [40]. Relaxor could be classified into two states: non-ergodic and ergodic [41]. Non-ergodic one can be transforms irreversibly into the ferroelectric state and ergodic does reversibly. Several material properties distinguish normal and relaxor ferroelectrics are summarized in Table 1 and below:

(i) The sharp well-defined phase transition temperature (Curie temperature) found for normal ferroelectrics is absent for relaxors. The dielectric constant maximum does not distinguish the exact paraelectric to ferroelectric phase transition as in normal ferroelectrics. The paraelectric to ferroelectric phase transition becomes broad and diffuse in relaxor and Curie ranges replace the Curie temperature. The permittivity of a relaxor is also dispersive in nature at radio frequencies, where

the permittivity decreases and the temperature of the dielectric constant maximum (T_m) shifts to higher temperature with increasing frequency.

(ii) In relaxor ferroelectrics, the dielectric constant does not follow Curie-Weiss law behavior above the ferroelectric transition. Instead, relaxers follow Curie-Weiss square law (sometimes called the quadratic Curie-Weiss law):

$$\frac{1}{\varepsilon_r} - \frac{1}{\varepsilon_m} = \frac{(T-T_m)^2}{C'} \tag{2.4}$$

where ε_r is the relative dielectric constant, ε_m is the dielectric constant maximum, T_c is the temperature of the dielectric constant maximum and C' is the modified Curie-Weiss constant. This quadratic relation is valid for materials that display diffuse phase transitions. Most materials; however, show intermediate behavior between the linear and quadratic limits. Uchino et al. proposed a variation power law as the modified Curie-Weiss law [41]

$$\frac{1}{\varepsilon_r} - \frac{1}{\varepsilon_m} = \frac{(T-T_m)^\gamma}{C'} \tag{4}$$

where γ is the critical exponent. The value of the critical exponent can vary from $\gamma = 1$, for purely normal ferroelectrics, to $\gamma = 2$, for purely relaxor ferroelectrics. The qualitative method to determine the parameter of relaxor ferroelectric is by plotting the inverse dielectric constant as a function of temperature as a log-log scale.

(iii) Another feature which distinguishes normal and relaxor ferroelectrics is the behavior of polarization. The relatively rapid decrease of the polarization to zero is found in normal ferroelectrics at T_c. This gradual decrease extends to temperature above T_m before reaching zero. This can be observed in P-E hysteresis loops. At temperatures well below T_m, relaxors show a typical P-E hysteresis loop; however, the loops decay slowly into simple non-linearity as the temperature increases through the Curie range.

(iv) Asthe temperature decreases, the number of polar region increases so that the regions are in contact; however, since these regions are oriented along different

polarization directions the crystal still appears isotropic. Several characteristics are caused by the polar regions orienting along difference axes. First, relaxor ferroelectrics exhibit weak remnant polarization. Second, due to the long coherence length of XRD, relaxor ferroelectrics appear cubic since they do not exhibit x-ray peak splitting. Third, under optical microscopy, relaxor ferroelectrics exhibit negligible birefringence [42].

Antiferroelectric

An antiferroelectric crystal is defined as a crystal whose structure can be considered as being composed of two sublattices polarized spontaneously in antiparallel directions and in which a ferroelectric phase can be induced by applying an electric field. Experimentally, the reversal of the spontaneous polarization in ferroelectrics is observed as a single hysteresis loop, and the induced phase transition in antiferroelectrics as a double hysteresis loop (Figure 6), when a low-frequency ac field of a suitable strength is applied [43].

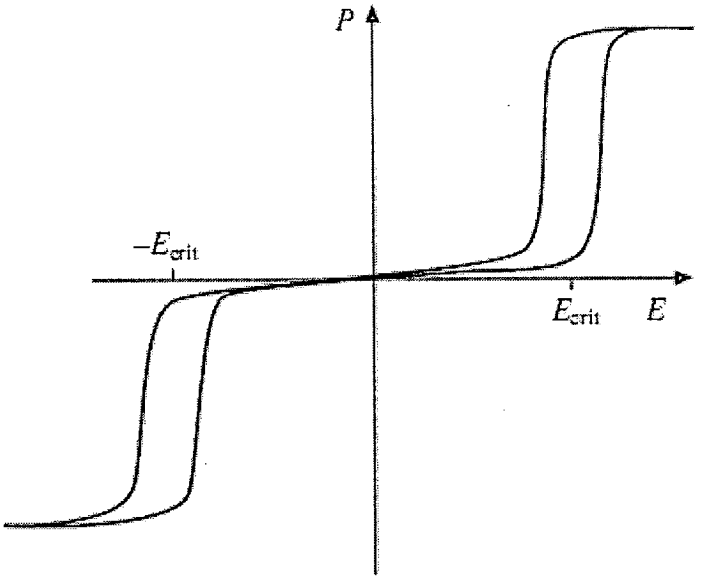

Figure 6 Antiferroelectric hysteresis loop [43]

Table 1 Differentproperty of normal and relaxor ferroelectrics [36]

Properties	Normal ferroelectrics	Relaxor ferroelectrics
Permittivity temperature dependence $\varepsilon_r = \varepsilon_r(T)$	Sharp 1st or 2nd order phase transition at Curie temperature (T_c)	Broad-diffuse phase transition around Curie maximum (T_m)
Permittivity temperature and frequencydependence $\varepsilon_r = \varepsilon_r(T, \omega)$	Weak frequency dependence	Strong frequency dependence
Permittivity behavior in paraelectric range ($>T_c$)	Follow Curie-Weiss law $\varepsilon_r = C/(T = T_0)$	Follow Curie-Weiss square law $1/\varepsilon_r = 1/\varepsilon_m + (T-T_m)^2 /2\varepsilon_m\delta^2$
Remnant polarization	Strong remnant polarization	Weak remnant polarization
Scattering of light	Strong anisotropy (birefringent)	Very weak anisotropy to light (pseudo-cubic)
Diffraction of X-ray	Line splitting owing to spontaneous deformation from paraelectric to ferroelectric phase	No X-ray line slitting giving a pseudo-cubic structure

Paraelectric

Paraelectricity is the ability of many materials (specifically ceramic crystals) to become polarized under an applied electric field. Unlike Ferroelectricity; this can happen even if there is no permanent electric dipole that exists in the material, and removal of the fields results in the polarization in the material returning to zero, as shown in Figure 7. The mechanisms which give rise to paraelectric behavior are the distortion of individual ions (displacement of the electron cloud from the nucleus) and the polarization of molecules or combinations of ions or defects. Paraelectricity

occurs in crystal phases in which electric dipoles are unaligned (i.e. unordered domains that are electrically charged) and thus have the potential to align in an external electric field and strengthen it. In comparison to the ferroelectric phase, the domains are unordered and the internal field is weak. The $LiNbO_3$ crystal is ferroelectric below 1430 K, and above this temperature it turns to paraelectric phase. Other perovskites similarly exhibit paraelectricity at high temperatures [44].

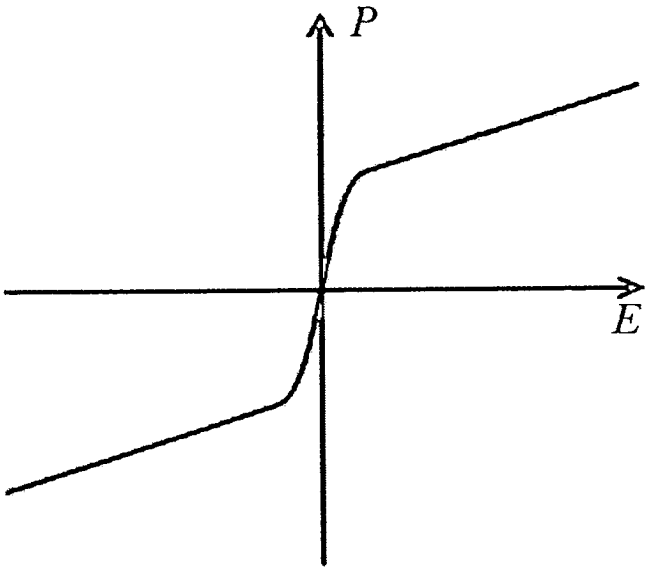

Figure 7 Paraelectric hysteresis loop [44]

Morphotropic Phase Boundary (MPB)

An MPB can be located at the compositional boundary between two perovskite materials with different symmetries by controlling the ratio of each perovskite component. The most common example of this phenomenon is the solid solution of lead zirconate-titanate, or $Pb(Zr_xT_{1-x})O_3$ (PZT). In fact, PZT is the most analyzed system with an MPB due to its exceptionally large and constant piezoelectric properties. This is due to the fact that PZT shows a nearly vertical, temperature independent, phase boundary between the $PbTiO_3$ (tetragonal) and $PbZrO_3$ (rhombohedral) phases at a composition of x~0.52, as shown in Figure 8 [45]. The origin for this maximization of the piezoelectric response in this MPB region is generally explained by the high degree of freedom for the electric dipoles.

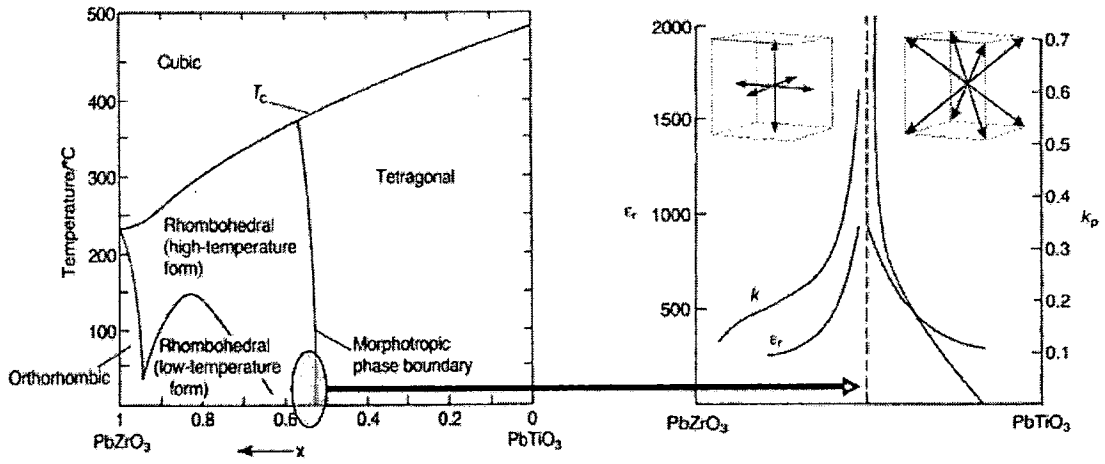

Figure 8 Phase diagram and piezoelectric properties for $Pb(Zr_xTi_{1-x})O_3$ceramic [45]

This allows them to be easily oriented via an electric field in a large number of directions, essentially combining the possible orientations of tetragonal (6 along [001]) with those of rhombohedral systems (8 along [111]). Domain systems arising can orient along all of these directions and form a more highly oriented polycrystalline sample under optimal poling. More recent structural studies also indicate another possibility, that an intermediate phase of monoclinic symmetry may exist at the MPB composition and results in the enhancement of piezoelectric and dielectric properties [46]. Although many lead free systems are described as having an MPB, usually the phase transition observed is not highly independent of temperature, with fairly wide ranges of compositions and the resulting enhancement of properties is not as compelling. These transitions are more aptly described by the term polymorphic phase transition.

Typical methods to synthesize ceramics

Solid-state reaction method

Solid-state reaction method is the most widely used method for the preparation of polycrystallinesolids from a mixture of solid starting materials. This method involves chemical decomposition, where solid reactants are heated to produce a new solid and normally use simple oxides powders such as carbonates, hydroxides, nitrates, sulfates, acetates, oxalates, alkoxides and other metal salts for

preparation. The solids do not react together at room temperature over normal time scales and it is necessary to heat them to much higher temperatures, often to 1000 to 1500 °C in order for the reaction to occur at an appreciable rate.An example of reaction between barium carbonate and titanium oxide at high temperature produce barium titanate by using solid-state reaction method.

$$BaCO_3(s)+TiO_2(s)\text{-- (}\sim 1200\ ^\circ C)\text{----->}BaTiO_3(s)+CO_2(g) \quad (5)$$

Solid-state reactions generally have an advantage in terms of production cost. However, it is commonly understood that the conventional solid state method requires compulsory grinding of different oxide mixtures for long periods of time as well as sintering. In addition, the synthesized component distributions are not homogeneous and particle sizes are relatively large [47, 48].

Sol-gel processing

Sol-gel process is a method for producing solid materials from small moleculesin a solution (sols) agglomerate and under controlled conditions eventually link together to form a coherent network (gel). The method is used for many applications in synthesis of novel materials. The advantages of the sol-gel process in general are high purity, homogeneity and low temperature. For a lower temperature process, there is a reduced loss of volatile components are thus the process is more environmental friendly. In addition, some materials that cannot be made by conventional means because of thermal and thermodynamically instability can be made by this process. However, the disadvantages are also real. The starting materials can be fairly expensive [49, 50].

Co-precipitation method

Co-precipitation (CPT) is the carrying down by a precipitate of substances normally soluble under the conditions employed. This method proceeds in two stages. First stage, the impurity is trapped either on the surface or inside the growing particles. If the growing particles have a crystal structure, then the impurity will become localized at regions of the solid phase with a perfect structure. During rapid precipitation, the growing particles will trap non-equilibrium impurities, which are usually in homogeneously distributed through the volume of the solid phase.

In the second stage, the concentration of defects within the precipitate decrease and the particles are flocculated. Impurities trapped during the first stage return either partially or completely to the medium. The concentration of impurities in the solid phase becomes equalized. The crystals acquire an equilibrium composition that depends only on the composition and temperature of medium [49, 50].

Hydrothermal synthesis method

Hydrothermal synthesis is generally defined as crystal synthesis or crystal growth under high temperature and high pressure water conditions from substances which are insoluble in ordinary temperature and pressure (<100 °C, <1 atm). Advantages of the hydrothermal synthesis method include the ability to synthesis crystals of substances which are unstable near the melting point, and the ability to synthesis large crystals of high quality. Disadvantages are the high cost of equipment and the inability to monitor crystals in the process of their growth. Hydrothermal synthesis can be affected both under temperatures and pressures below the critical point for a specific solvent above which differences between liquid and vapour disappear, and under supercritical conditions. The solubility of many oxides in hydrothermal solutions of salts is much higher than in pure water; such salts are called mineralizers. There is also a group of solvothermal synthesis methods, relational to hydrothermal methods; this group of methods is based on the use of organic solvents and supercritical CO_2.

Combustion technique

Combustion techniqueuses the energy released from the oxidation-reduction reaction. It has emerged as an important technique for the synthesis and processing of advanced ceramics, which involves a self-sustained reaction between reaction materials and fuel (e.g., urea, glycine, citric acid, alanine or carbohydrazide). The advantages of this technique include inexpensive precursors, simple preparation process, and resulting good electrical properties with lower firing temperature and shorter dwell time [24, 25, 26].

I. Types of organic compounds

Hwang et al. [52] has investigated decomposition of the five fuels by Thermogravimetric analysis. They choose the fuel such as glycine, urea, alanine, citric acid or carbohydrazide. Some properties of five fuelsthey select are shown in Table

2.The results of the thermal analysis show that there were different weight losses of organic fuels. When using carbohydrazide as organic fuel, indicating that the chemical reaction took place very rapidly. But remaining weight is 22% of its original weight. While using glycine and alanine as organic fuels, the thermogravimetric of both demonstrated similar results. Their reactions are very fast and remaining weight lower than 10%. When using urea and citric acid as organic fuels, the chemical reaction was not rigorous when compared with glycine and alanine.

II. Influence of fuels and development of novel synthesized combustion technique of powders and ceramics

The crystal structure and microstructure of Ni-Zn ferrites prepared by combustion technique with various organic fuels was studies by Hwang et al. [52]. They result show that the pure phase of Ni-Zn was obtained while using glycine, alanine and corbohydrazide. While using urea and citric as organic fuels, the impurities phase was obtained existed in the diffraction pattern, as seen in Figure 10. The nanocrystalline sizes are ranging between 20.2 and 43.7 nm, as seen in Table 3. The results indicated that the ceramic synthesized by the combustion technique produced nanocrystalline sizes.

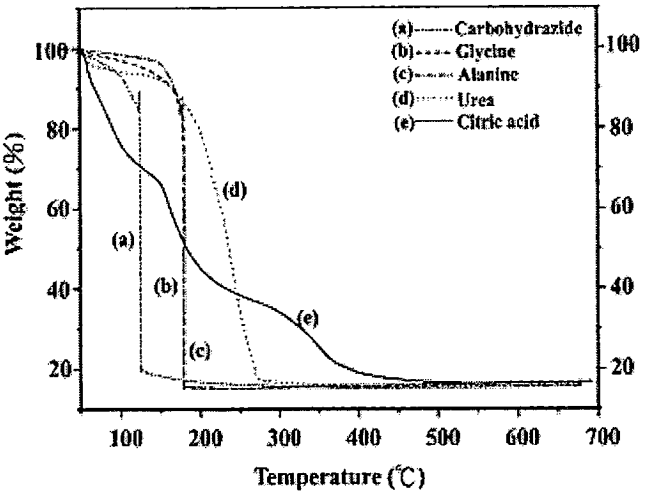

Figure 9 Thermogravimetric of fuel [52]

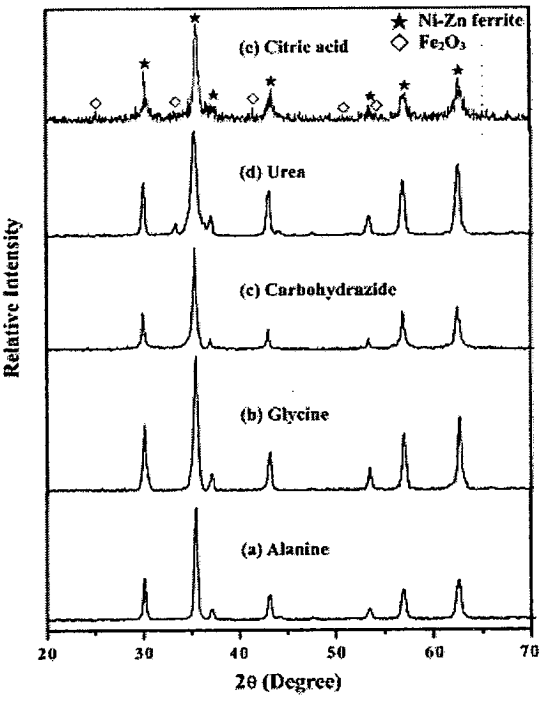

Figure 10 XRD patterns of the Ni-Zn ferrites with various organic fuels: (a) alanine (b) glycine (c) carbohydrazide (d) urea and (d) citric acid [52]

Our group successfully fabricated ceramics oxide by the combustion technique such as $Pb_{1-x}Ba_xTiO_3$(PBT), $(Ba_{0.25}Sr_{0.75})(Zr_{0.75}Ti_{0.25})O_3$ (BSZT)etc. [20, 22]. In the case of PBT, the result show that the combustion technique produced nano-powders of PBT powders, with average size around 54-77 nm, as seen in Figure 11. A high density above 96.5% with calcined between 1,000 and 1150 °C and sintered between 1200 and 1250 °C for only 2 h can be prepared by the combustion technique, which shorter time than prepared by the solid state reaction method. In the case of $(Ba_{0.25}Sr_{0.75})(Zr_{0.75}Ti_{0.25})O_3$, it was synthesized using combustion technique compared with solid state reaction method. The results shown that the particle size of BSZT powder prepared via the combustion technique is 0.13-0.30 μm and the solid state reaction method is 0.18-0.38 μm. Moreover, the result shows that the combustion technique has potential to reduce the calcination temperature and is suitable for prepared oxide ceramic. Therefore, the combustion method was chosen for preparation BNKFT, BNKNT and BNKLT ceramics in this work.

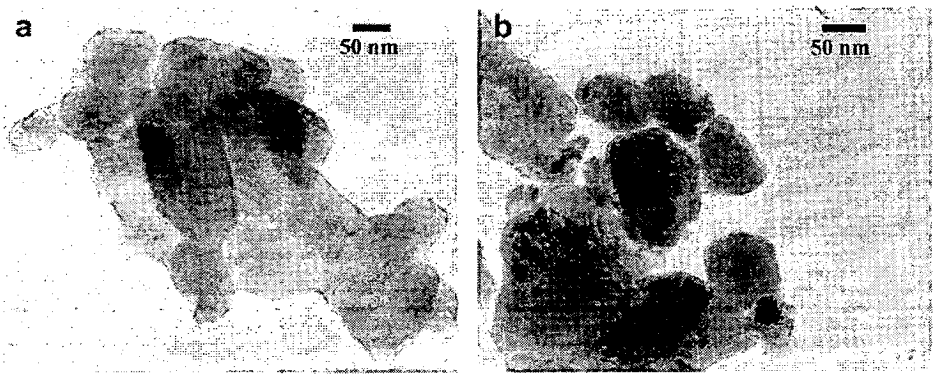

Figure 11 TEM micrographs of (a) original magnification x120,000 of $Pb_{0.60}Ba_{0.40}TiO_3$ powder calcined at 1050 °C and (b) original magnification x100,000 of $Pb_{0.20}Ba_{0.80}TiO_3$ powder calcined at 1150 °C [20]

Table 2 Someproperties of organic compounds [52]

Properties	Organic component				
	Alanine	Glycine	Carbohydrazide	Urea	Citric acid
Structure formula	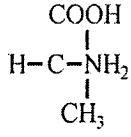		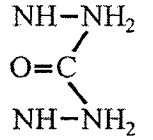	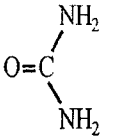	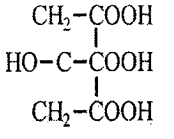
Molecular weight (g/mol)	80.1	90.1	75.1	60.1	192.1
Heat of combustion (kJ/g)	18.2	13.0	12.6	10.5	10.2
Decomposition temperature (°C)	314	262	153	135	175

Table 3 Effect of various fuels of the Ni-Zn ferrites prepared by the combustion technique [52]

Fuel	T_m[a] (°C)	Amount of gas produced (mole)	Crystallite size[b] (nm)	Surface area (m^2/g)	Carbon content (wt.%)	$Ni^{2+}:Zn^{2+}:Fe^{3+}$	M_s[C] (Am^2/kg)
Alanine	1245	20.7	38.6	24.7	1.64	0.500:0.467:1.920	60.8
Glycine	1150	26.2	32.7	31/2	1.53	0.500:0.471:1.922	62.4
Carbohydrazide	1380	24.0	43.7	20.6	1.87	0.500:0.462:1.917	58.5
Urea	785	30.7	20.2	48.5	3.82	0.500:0.483:1.936	57.2
Citric acid	725	26.2	22.7	44.1	5.75	0.500:0.490:1.947	55.8

Note: [a]T_m the maximum combustion temperature, measured by Pt-Pt-Rh thermocouple.

[b] Crystalline size of the as-synthesized Ni-Zn ferrite powders calculated from the line broadening of the (311) XRD peak by Sherrer formula.

[c]M_s the saturation magnetization of the sintered Ni-Zn ferrite samples (950 °C/2h).

One Component Systems

Useful lead-free materials are often binary or ternary solid solutions. Before discussing these more complex material systems in next section, this section introduces and discusses the member compositions of based ceramics.

$(Bi_{0.5}Na_{0.5})TiO_3$ (BNT)

Since BNT was discovered by Smolenskii et al. in 1960 [2, 53], it has gained a lot of attentions from various aspects. It has high Curie temperature (T_c=320°C). Recently, detailed studies on the structure transformation of BNT single crystals have been carried out by Hiruma et al. using x-ray diffraction. They found that the pure

BNT is a perovskite-structured ferroelectric with rhombohedral symmetry at room temperature (RT), and its phase transitions are complicated [54]. The phase transition temperatures T_{R-T} from rhombohedral to tetragonal and T_{T-C} from tetragonal to cubic are approximately 230 and 320°C upon heating, respectively, for BNT single crystals. Lee et al. [55] studies the lattice parameter of BNT ceramic system calculated by the Rietveld method with XRD patterns, and they reported that the lattice constants of BNT ceramics are a=3.888 Å.

Lencka et al. [56] studied the microstructure of BNT powder prepared by hydrothermal method, were investigated using field emission scanning microscopy (FESEM), x-ray diffraction (XRD) and specific surface areas were measured by multipoint BET technique. The average particle size calculated from FESEM range from 40 and 150 nm can be seen in Figure 12. Crystallite sizes calculated from the XRD peak broadening range from 13 to 28 nm. The measured specific surface areas range from 20.0 m^2/g to 27.6 m^2/g.Saradhi et al. [57] investigated the grain size of BNT ceramics prepared by conventional double sintering method and analyzed by scanning electron microscope (SEM). They revealed that the average grain size ranged from 1 to 3 μm, corresponding to the result of Zuo et al. [50].

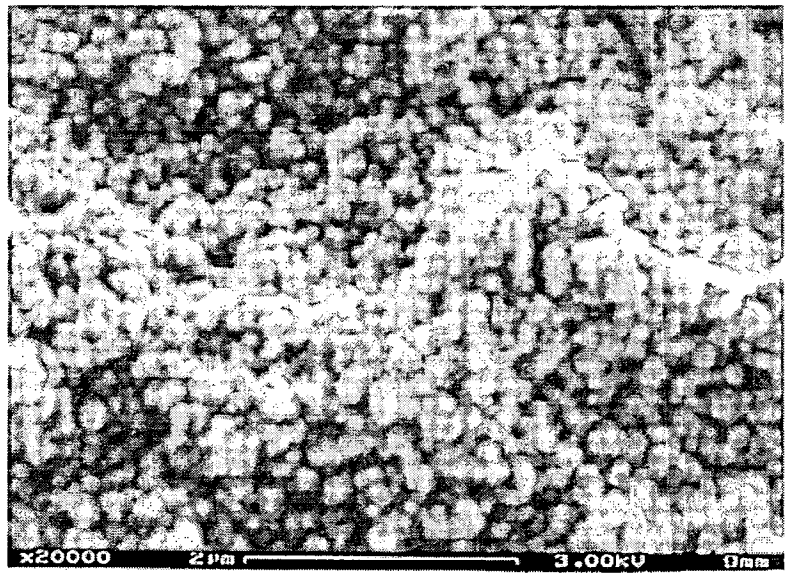

Figure 12 FESEM micrograph of the BNT powders [57]

The temperature dependences of the dielectric constant (ε_s) and the loss tangent (tanδ) from 20 Hz to 1 MHz of BNT ceramics between RT and 500 °C are shown in Figure 13. There are two dielectric peaks anomalies. The appearance of first temperature peak (T_d) is caused by the phase transition from rhombohedral ferroelectric to tetragonal anti-ferroelectric phase. The appearance of second temperature peak (T_m) can be explained by the transition from tetragonal anti-ferroelectric to cubic paraelectric phase T_d and T_m occurred in a temperature at 187 °C and 325 °C. The tan δcurves of the BNT reveal only one peak near the temperature of T_d and tan δ sharply increases when temperature is higher than T_m [54].

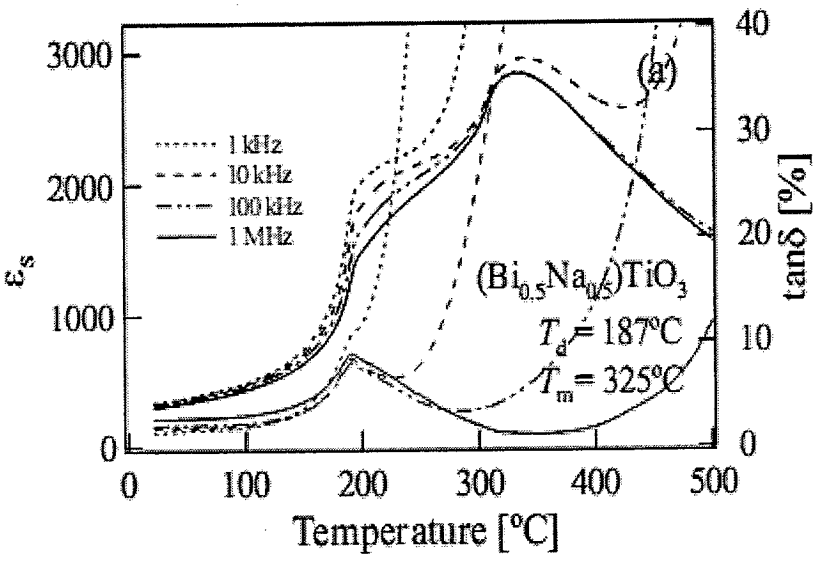

Figure 13 Temperature dependences of dielectric constant (ε_r) and loss tangent (tanδ) in temperature range from RT to 500 °C of BNT ceramics [54]

The BNT ceramics shows the strong ferroelectric property of a large remnant polarization and relatively high piezoelectric properties compared with other lead-free piezoelectric ceramics. Zuo et al. [58] reported that the remnant polarizations, piezoelectric constant and coupling factor of BNT are 38 $\mu C/cm^2$, 75 pC/N and 15.4 %. Nevertheless, the applications of BNT are limited by its high coercive field and its high conductivity. Coercive fields vary greatly between 2 kV/mm for sol-gel derived BNTand 7.3 kV/mm for BNT prepared by a mixed oxide route [59]. To solve

these problems and improve the electric properties, various types of compounds were added into BNT to form solid solution, such as $BaTiO_3$, $SrTiO_3$, $CaTiO_3$, $Bi_{0.5}K_{0.5}TiO_3$, $NaNbO_3$, $Ba(Cu_{0.5}W_{0.5})O_3$, and discussing complex material in next section.

$(Bi_{0.5}K_{0.5})TiO_3$ (BKT)

BKT was first determined to be ferroelectric by Smolenskii et al. [60], which was found in 1961 at the same time as BNT. Its unit cell is similar is that if BNT but with all the sodium ions replaced by potassium ions. It is a tetragonal ferroelectricperovskite at room temperature and a relatively high Curie temperature T_c of 380 °C. Above the Curie temperature BKT is cubic paraelectric [61]. Ivanova et al. [62], reported the lattice parameter of BKT as a = 0.3913 nm, c = 0.3990 nm at room temperature.

SEM micrograph of BKT powder was studied by Hou et al. [63], and they reported that the particles size was very small and relatively uniform, as can be seen in Figure 14. The average particle size was between 100 and 200 nm. FESEM micrograph of the BKT powders demonstrated a uniform spherical particle with the diameter ranges from 40 to 150 nm, which was studies by Lencka et al. [56], as shown in Figure 15.

The dielectric constant (ε_r) and dielectric loss ($\tan\delta$) of BKT ceramics were studied by Hiruma et al. [64]. The ε_r and $\tan\delta$ at room temperature of BKT are 524 and 6.8% at 1MHz. Some authors showed the values of room temperature dielectric constant ε_r and loss tan δ at 1 kHz are 733 and 4.8 %. Yang et al. [65] studies the dielectric relaxer properties of ferroelectric BKT single crystal by molten salt method. They reported that the maximum in ε_r is diffusive and centered at around 357 °C accompanied by a strong dispersion of dielectric maximum temperature (T_m) with frequency. Upon increasing the field frequency, the dielectric maximum decreases, while the Curie temperature increases (from 337 C at 1 kHz to 362 at 1000 kHz), showing the relaxer behavior of the present ceramics, as shown in Figure 16.

The polarization hysteresis behavior of BKT measured at several temperatures was also reported, as shown in Figure 17. Hysteresis loop is observed even at temperatures as high as 260 °C [64]. As expected, the coercive field also

gradually decreases with an increase in temperature, as does the remnant polarization. The remnant polarization (P_r = 22.2μC/cm^2) and 52.5 kV/cm of BKTwere reported [66].

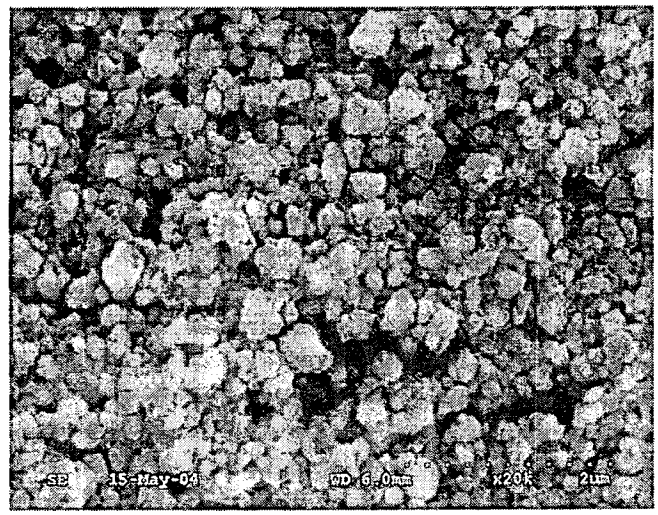

Figure 14 FESEM micrograph of the BKT powders was studied by Hou et al. [63]

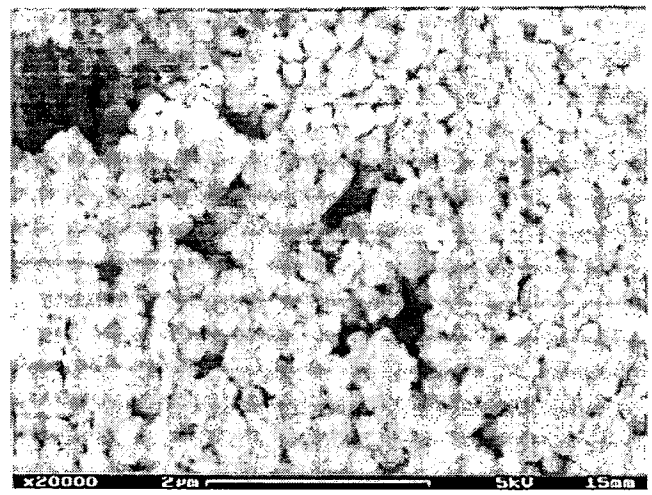

Figure 15 FESEM micrograph of the BKT powders was studied by Lencka et al. [56]

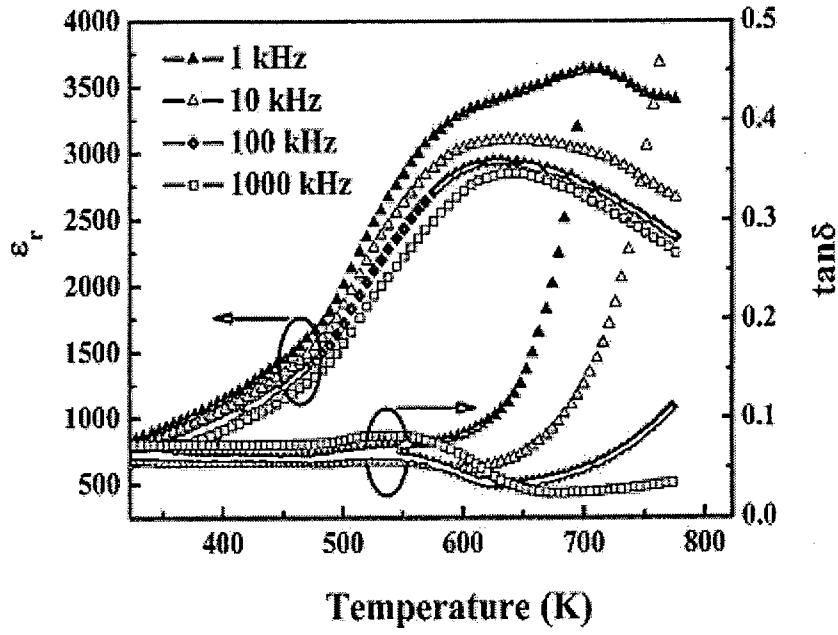

Figure 16 Temperature dependence of dielectric constant ε_r and loss tanδ at various frequencies for $(K_{0.5}Bi_{0.5})TiO_3$ ceramics [65]

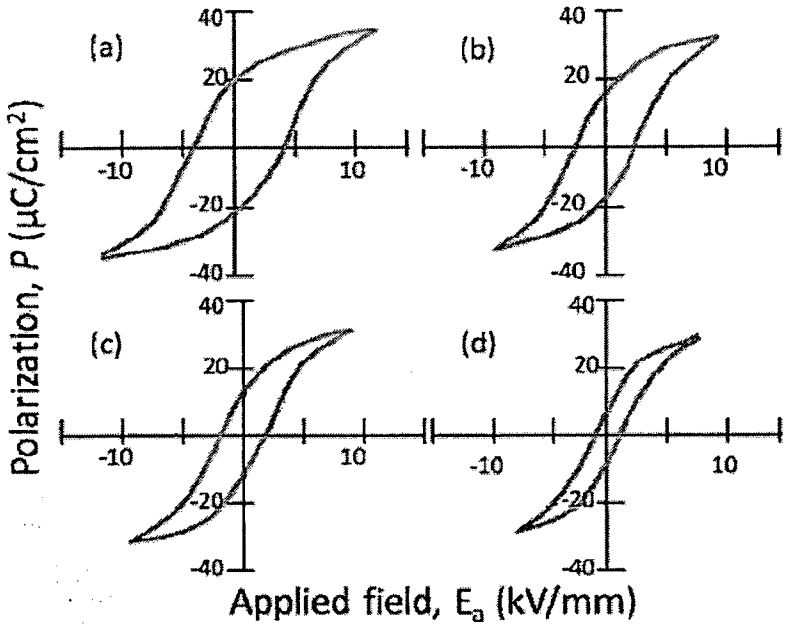

Figure 17 Polarization of KBT measured at temperatures of (a) 100 °C, (b) 200 °C, (c) 240 °C and (d) 260 °C [66]

Binary Systems

For some of the lead-free systems described above, the piezoelectric properties are enhanced through the use of dopants. The enhancement of piezoelectric properties is selection of a composition near an MPB in a solid solution. This section discusses the structure and properties of several lead-free binary solid solution material compositions.

$Bi_{0.5}Na_{0.5}TiO_3$ –$BaTiO_3$ (BNT-BT)

$BaTiO_3$ (BT) has also been combined in a solid solution with BNT, in which case an MPB is found at 6-7 mol% BT between the ferroelectric rhombohedral and ferroelectric tetragonal phases, as shown in Figure 18. At this composition, the system exhibits improved properties relative to BNT, such as the piezoelectric constant (d_{33}=125 pC/N), coupling factor (k_p=20%), and dielectric constant (ε_r=580) [67].

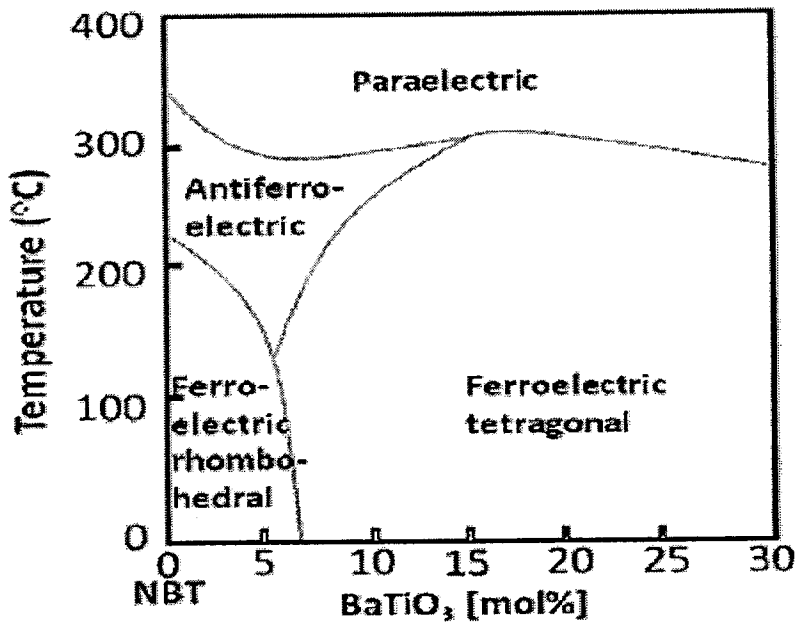

Figure 18 Phase diagram of BNT-BT showing the MPB between the ferroelectric rhombohedral phase and the ferroelectric tetragonal phase, reproduced from Takenaka et al. [67]

$Bi_{0.5}Na_{0.5}TiO_3$ –$NaNbO_3$ (BNT-NN)

BNT was also combined with $NaNbO_3$ (NN) by Li et al. [6]. They reported that the solid solution of BNT-NN forms MPB between rhombohedral ferroelectric and orthorhombic anti-ferroelectric structure in the region of 2-8 mol% NN. At the MPB, the dielectric constant at RT, dielectric loss tangentat RT, piezoelectric constant and electro mechanical coupling factor varies from 467-889, 4.11-6.26 %, 31-88 pC/N and 12.3-17.9%. Furthermore, the BNT-NN ceramics exhibited relaxer behavior which is characterized by a diffused phase transition, as shown in Figure 19.

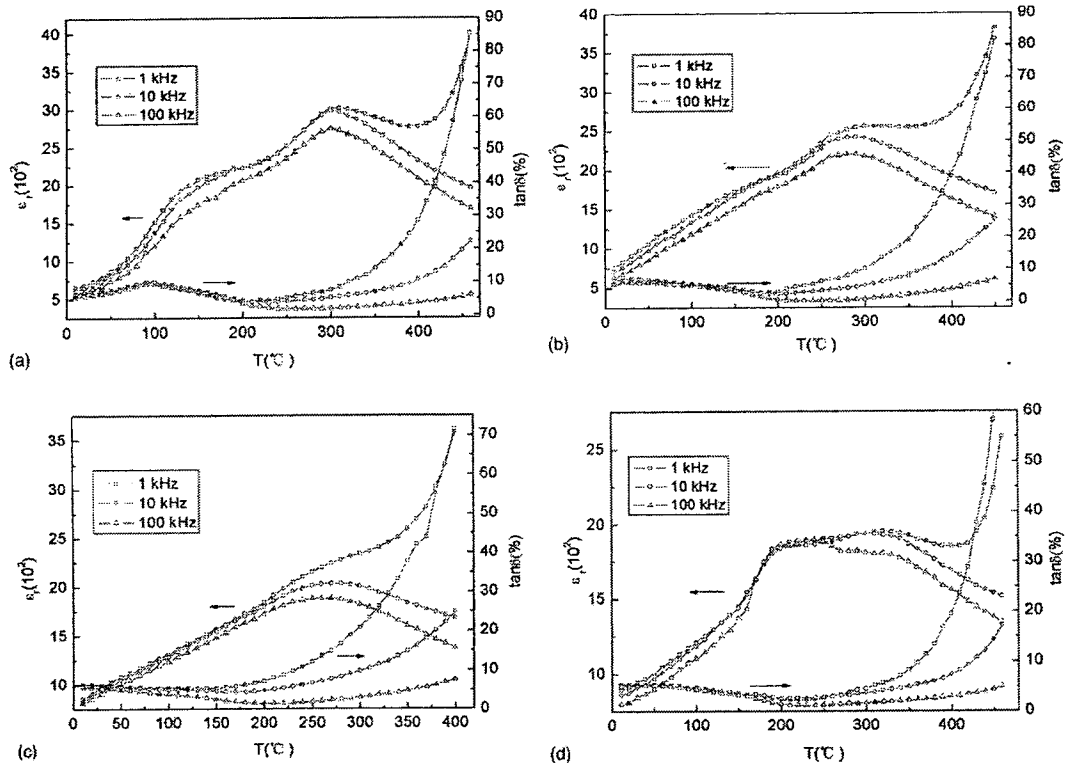

Figure 19 Temperature dependence of dielectric constant (ε_r) and dielectric loss (tanδ) for (1-x)NBT–xNN ceramics at 1, 10, 100 kHz with (a) x = 0.02, (b) x =0.04, (c) x =0.06 and (d) x =0.08[6]

$Bi_{0.5}Na_{0.5}TiO_3$ –$Ba(Cu_{0.5}W_{0.5})O_3$ (BNT-BCW)

For the BNT-BCW system, the structure remains a single rhombohedral phase with no MPB seen within the addition amount of BCW from 0 to 6 mol%. The addition of BCW into BNT ceramics facilitated the poling process by a reduction in leakage current. 0.995BNT-0.005BCW ceramics exhibit a relatively high piezoelectric electric constant (d_{33}=80 pC/N), electromechanical coupling factor (k_p=18.1%), dielectric constant (ε_r = 328) and a relatively low dielectric loss (tanδ = 0.015) [68].

$Bi_{0.5}Na_{0.5}TiO_3$ –$SrTiO_3$ (BNT-ST)

BNT was also combined with ST by Watanabe et al. [7], showing an increase in the dielectric constant compared to undoped BNT, as shown in Figure20. T_d, T_m and T_{R-T} of BNT-ST ceramics was found that it shifts the lower temperature when the ST content increased as shown in Figure 21. The optimum values of d_{33} is 133 pC/N obtained from 0.80BNT-0.20ST ceramics.

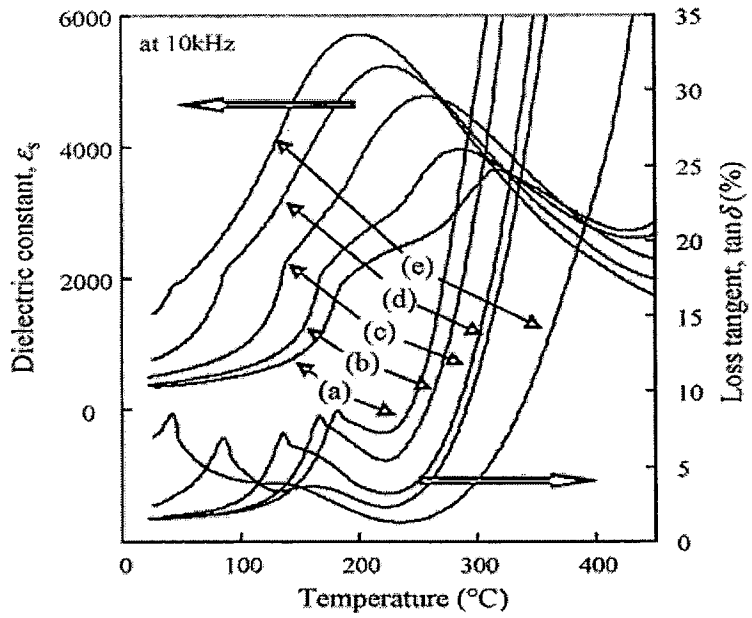

Figure 20 The dielectric constant and tanδ of BNT-ST (a) x = 0.04, (b) x = 0.08, (c) x = 0.14, (d) x = 0.20 and (e) x = 0.24[7]

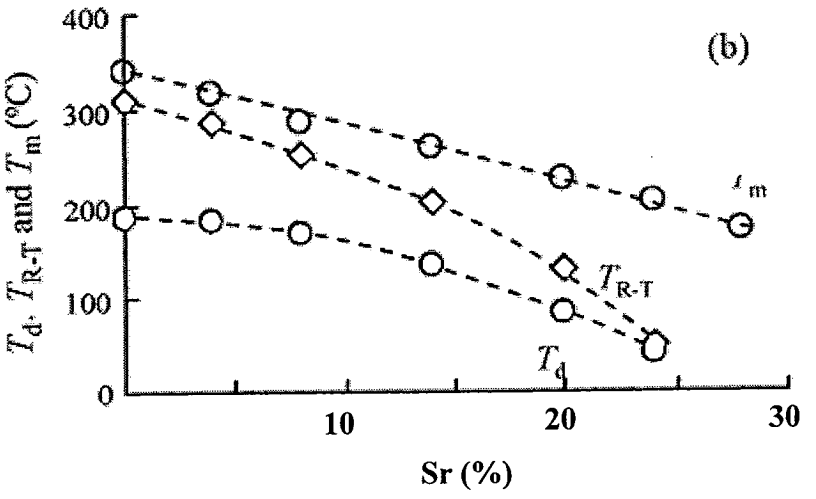

Figure 21 T_d,T_{R-T} and T_m of BNT-ST ceramics[7]

$Bi_{0.5}Na_{0.5}TiO_3$-$Bi_{0.5}K_{0.5}TiO_3$ (BNT-BKT)

The crystal structure of BNT-BKT ceramics was studied by Yang et al. [1]. They reported that a solid solution of BNT-BKT forms MPB between rhombohedral and tetragonal structure in the region of 16-22 mol % BKT. It agrees with the results of Sasaki [69].The addition of BKT into BNT ceramic caused the grain size to decrease. The density increases with increasing BKT content, the maximum density is obtained at18 mol% of BKT, as shown in Figure 22.

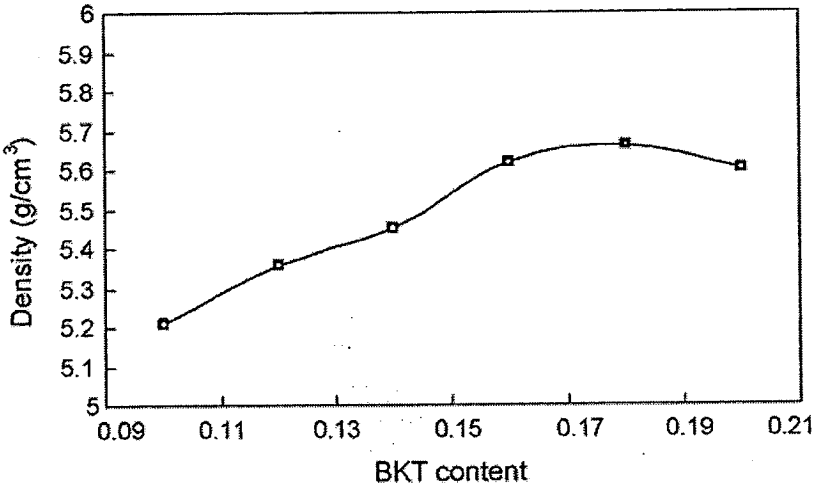

Figure 22 Density of BNT-BKT ceramics [1]

The dielectric constant (ε_r) and dielectric loss (tanδ) of BNT-BKT were also reported. The highconcentration of caused the ε_r increases andthe loss tanδ to decreased. There are two abnormal temperature peaks at around 100-200 and 300-350 °C were reported. Takenka et al. [70] concluded that these dielectric anomalies are attributed to ferroelectric-antiferroelectric and antiferroelectric-paraelectric phase transitions from the shape of P-E curve. Furthermore, BNT-BKT ceramics exhibited a relaxor ferroelectric behavior, as shown in Figure 23, agrees with the results of Yasuda and Konda [71].

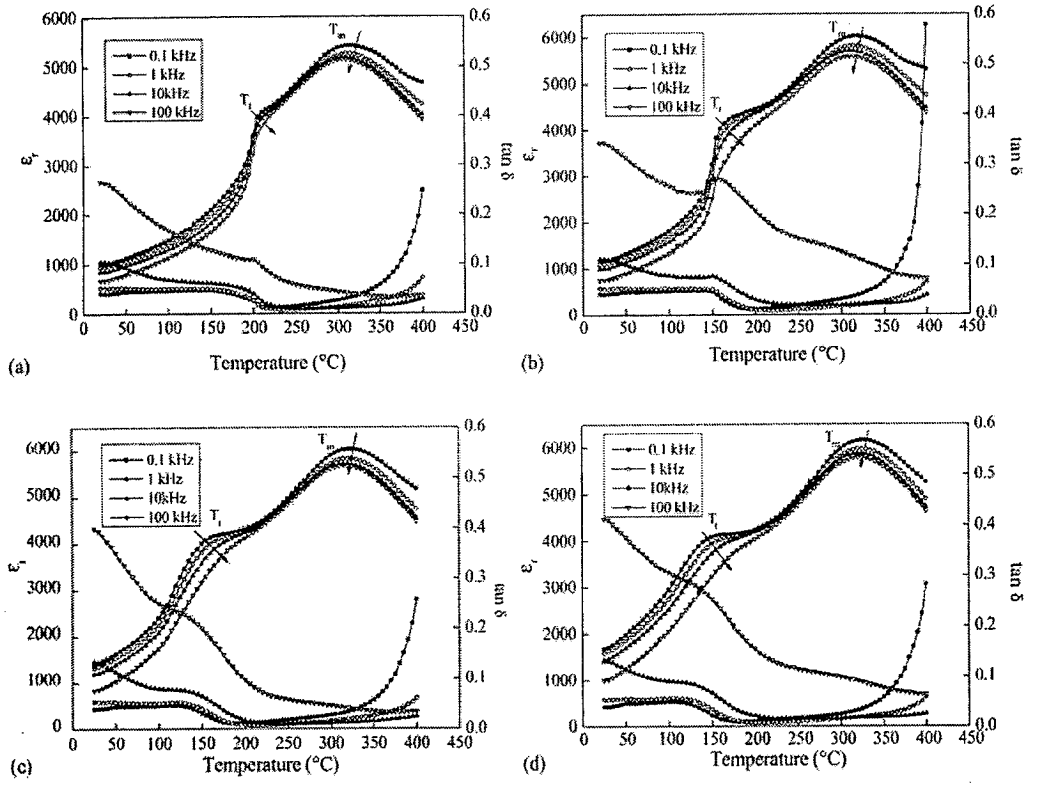

Figure 23 The dielectric constant and dielectric loss of BNT-BKT ceramics: (a) 12 mol% of BKT (b) 16 mol% of BKT (c) 18 mol% of BKT (d) 20 mol% of BKT[70]

The piezoelectric constant (d_{33}) and electromechanical coupling factor (k_p) of BNT-BKT were also reported. The addition of BKT into BNT ceramics increased d_{33} and k_p. The optimum values of d_{33} and $k_p$were found to be 144 pC/N, 29% at 18 mol% of BKT.

From the literature, the solid solution of BNT-BKT ceramics showed different piezoelectric properties. A comparison of the properties of BNT-BKT ceramics and BNT doping other of various groups is shown in Table 4.

Table 4 The optimal piezoelectric constant (d_{33}) and electromechanical coupling factor (k_p) of the composition in various BNT-based piezoelectric ceramics

BNT-based solid solution	MPB	d_{33} (μC/N)	K_p (%)	Ref.
BNT	-	58	12	[72]
$0.94BNT\text{-}0.06BaTiO_3$	o	125	20	[73]
$0.995BNT\text{-}0.005Ba(Cu_{0.5}W_{0.5})O_3$	o	80	18.1	[68]
$0.98BNT\text{-}0.02NaNbO_3$	-	88	17.9	[6]
$0.985BNT\text{-}0.01EuTiO_3$	-	46	-	[74]
$(Bi_{0.5}Na_{0.5})_{0.9742}La_{0.0172}TiO_3$	-	91	13	[75]
$0.98BNT\text{-}0.02BiScO_3$	-	74	14.4	[76]
$0.99BNT\text{-}0.01CaTiO_3$	-	50	13.8	[7]
$0.993BNT\text{-}0.007Bi(Mg_{2/3}Nb_{1/3})O_3$	-	94	-	[77]
$0.994BNT\text{-}0.006BaNb_2O_6$	-	94	-	[78]
$0.88BNT\text{-}0.12PbTiO_3$	o	106.6	33.2	[79]
$0.82BNT\text{-}0.18Bi_{0.5}K_{0.5}TiO_3$	o	144	29	[1]

Ternary Systems

As the binary systems described above still have many drawbacks and are not capable of replacing PZT in all of its applications, new lead-free compositions have become even more complex through the use of ternary solid solutions.

$Bi_{0.5}Na_{0.5}TiO_3$-$Bi_{0.5}K_{0.5}TiO_3$-$BiFeO_3$(BNT-BKT-BF)

Several reports have been made by Zhou et al. for the BNT-BKT-BF ternary system. The MPB in this system is between rhombohedral and tetragonal phases, where composition of $0.18<x<0.21$ and $0<y<0.05$ in (0.97-x)BNT-xBKT-0.03BF and (0.82-y)BNT-0.18BKT-yBF [18] respectively. Zou et al. [80] studied the microstructure of BNT-BKT-BF ceramics by SEM technique. They reported that the addition of BF into BNT-BKT caused bulk sample increased and promotegrain growth.

Measurement of the dielectric constant ε_r, piezoelectric constant d_{33} and the planar electromechanical coupling factor k_p of BNT-BKT-BF ceramics were studied by Zhou et al. [19]. The ε_r,d_{33} and K_p increased with increasing BF into BNT-BKT ceramics. The ceramics were found to exhibit a typical relaxor behavior. 0.79BNT-0.18BKT-0.03BF ceramics demonstrated the largest d_{33} and k_p are 170 pCN^{-1} and 36.6 %, as shown in Figure 24 (a) and (b) and Figure25, which shows that ceramics are very promising lead-free piezoelectric materials.

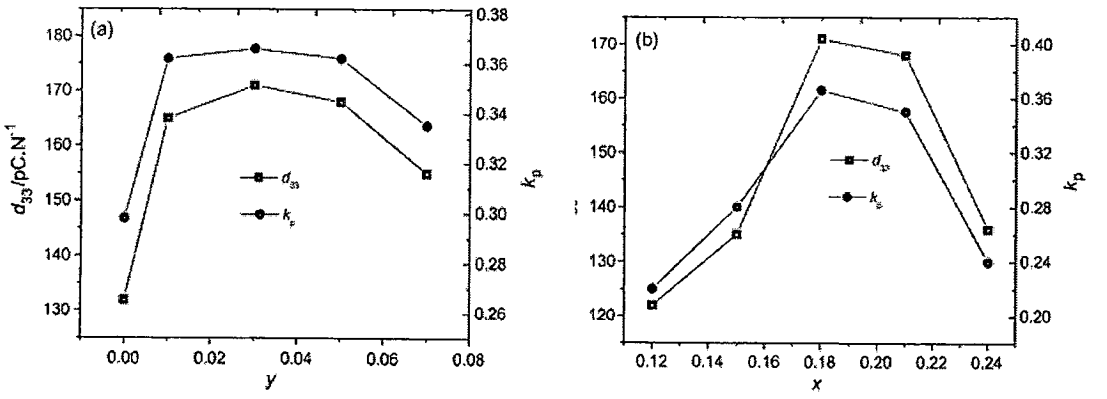

(a) (b)

Figure 24 Piezoelectric constant d_{33} and planar lectromechanical coupling factor k_p of (1−x−y)BNT–xBKT–yBF ceramics as a function of the amount of BKT and BF: (a) x = 0.18 and (b) y = 0.03 [19]

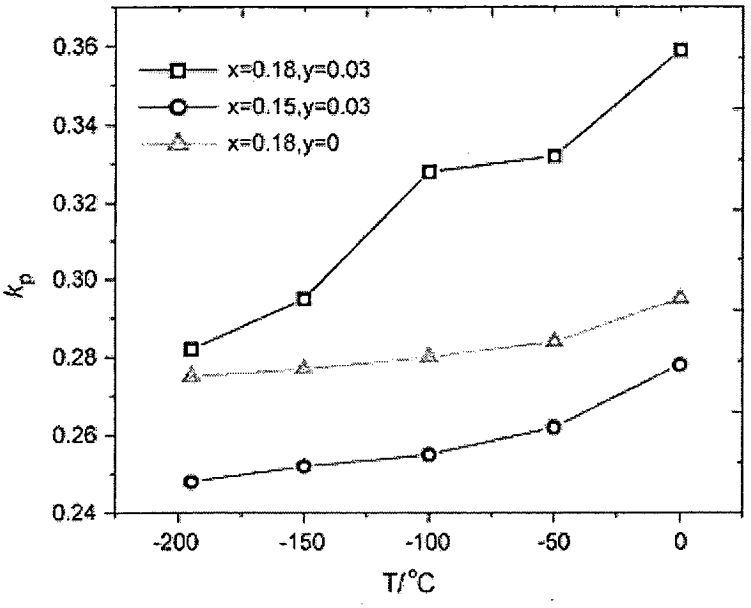

Figure 25 The electromechanical coupling factor k_p of (1−x−y)BNT–xBKT–yBF ceramics with x=0.18, y =0; x =0.18, y = 0.03 andx =0.15, y = 0.03 [19]

$Bi_{0.5}Na_{0.5}TiO_3$-$Bi_{0.5}K_{0.5}TiO_3$-$K_{0.5}Na_{0.5}Nb_{0.5}O_3$(BNT-BKT-KNN)

$K_{0.5}Na_{0.5}NbO_3$(abbreviated as KNN) is a well-known lead-free piezoelectric ceramic because of its high Curie temperature ~420 °C and large electromechanical coupling factors. Recently, Yao et al. [15] added a small amount of KNN to BNT-BKT. The phase transition between rhombohedral and tetragonal phases was confirmed. The piezoelectric properties of BNT-BKT-KNN were also reported 0.75 BNT-0.22BKT0.03KNN exhibited the d_{33} of 167 pC/N and k_p of 35.5%, as shown in Figure 26.

Hussain et al. [81] studied the bipolar strain behavior of KNN-modified BNT-BKT measured at 0.2 Hz under an applied electric field of 50 kV/cm. They have shown BNT-BKT without KNN exhibit a butterfly-shaped curve typical of ferroelectric material with maximum and negative strains of 0.12% and 0.11%, respectively. When a small amount of KNN is introduced, the curves change shape, resulting in an increase in maximum strain and a concurrent decrease in the negative strain. At 3 mol% KNN, a significant enhancement in strain (S=0.22%). Singh et al.

[82] studies the BNT-BKT-KNN ternary system by conventional solid state method. 0.80BNT-0.20BKT-0.01KNN exhibited the largest strain ever reported for a polycrystalline lead-free ceramics, ~0.80%, as shown in Figure 27, which is even higher than the strain obtained with established ferroelectric $Pb(Zr,Ti)O_3$ ceramics and is comparable to strains obtained in Pb-based antiferroelectrics.

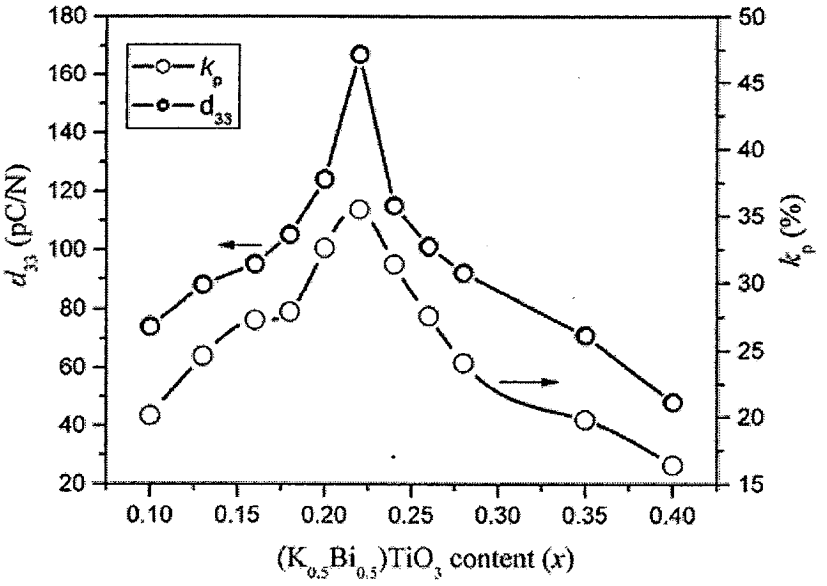

Figure 26 Piezoelectric coefficient d_{33} and planar coupling factor k_p of (1-x-y)BNT-xBKT-0.30KNN at x = 0.10–0.40 [15]

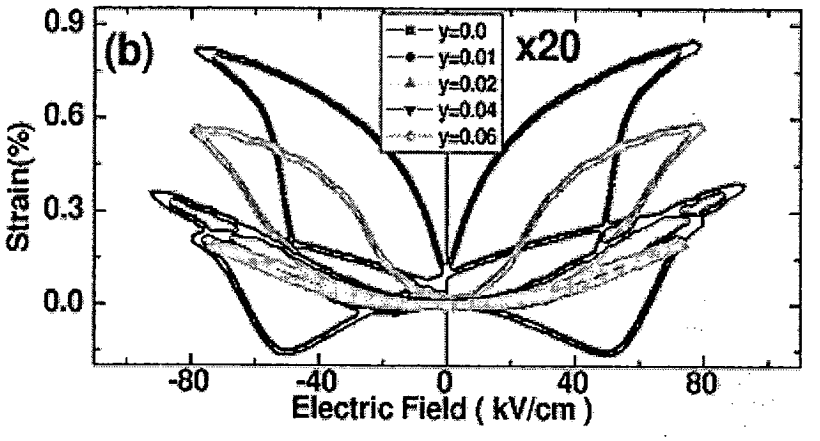

Figure 27 Bipolar strain vs electric field of 0.80BNT-0.20BKT 0.01KNN ceramic at room temperature at 1 Hz [82]

$Bi_{0.5}Na_{0.5}TiO_3$-$Bi_{0.5}K_{0.5}TiO_3$-$Bi_{0.5}Li_{0.5}TiO_3$(BNT-BKT-BLT)

Lin et al. [83] also studied the solid solution of BNT-BKT-BLT near the MPB. The ceramics were prepared by solid state reaction method and investigated by X-ray diffraction and for piezoelectric properties. The XRD patterns showed the MPB of therhombohedral phase and tetragonal phase. 0.70BNT-0.20BKT-0.10BLT demonstrated that the excellent piezoelectric constant and planar coupling factor of 231 pC/N and 41%, as shown in Figure 28. Hiruma et al. [84] added a small amount of KNN to BNT-BKT. The addition of BLT decreases greatly the sintering temperature and assists in the densification of BNT-BKT ceramics. The depolarization temperature (T_d) shows a strong dependence on the concentration of BLT and reaches the highest values at the MPB. These results show that the BNT-BKT-BLT ceramics are promising candidates for the lead-free materials.

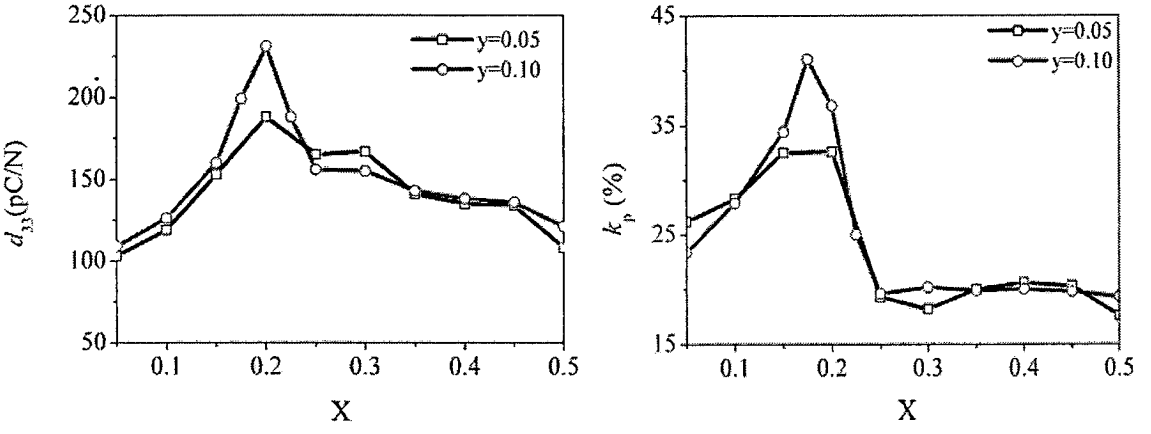

Figure 28 Variation of piezoelectric coefficient d_{33} and planar electromechanical coupling factor k_p with x for the (1-x-y)BNT-xBKT-yBLT ceramics (y=0.05 and 0.10) [83]